Observational Indications of Indirect Acidification in Asia: Enhanced Deposition of Nitric Acid Gas Expelled from the Aerosol Phase by Sulfate

Mizuo KAJINO*, Hiromasa UEDA**, Shinji NAKAYAMA** and Hirohiko ISHIKAWA

*COE researcher, DPRI, Kyoto University

**Acid Deposition and Oxidant Research Center, Niigata, JAPAN

Synopsis

Indirect acidification, i.e., enhancement of semi-volatile aerosol components deposition associated with increased SO_4^{2-} concentration has now been shown to occur in general air pollution, analyzing Acid Deposition Monitoring Network in East Asia (EANET) monitoring data collected at six stations in Japan. This effect was firstly detected as a result of volcanic SO_2 plumes (Satsumabayashi et al., 2004, Kajino et al., 2005). Results indicate that as SO_4^{2-} concentration increases, NO_3^- in aerosol phase is expelled, increasing the HNO_3 gas concentration. The deposition of HNO_3 gas occurs at a high velocity, consequently accelerating the deposition of NO_3^- despite a constant total (gas plus aerosol) nitrate concentration. In western Japan, this indirect acidification is most influential from spring to autumn, when the Asian continental outflow carries sulfate-rich contaminated air masses, but is not pronounced in the air masses containing abundant sea-salt particles and related cation components in aerosols.

Keywords: acid deposition, sulfate, nitrate, dry deposition, wet deposition

1. Introduction

Heterogeneous (gas and particles) and multiphase (gas and liquid phase) reactions play a major role in tropospheric chemistry, such as aerosol and oxidant formation, inducing health problems and environmental acidification (ex. Ravishankara, 1997; Finlayson-Pitts and Pitts Jr., 1997; Jang et al., 2002; Knipping and Dabdub, 2003; Laskin et al., 2003). Indirect acidification, which involves heterogeneous and multiphase chemistry, is a process of acid deposition acceleration associated with changes in gas-aerosol partitioning of semi-volatile aerosol components, such as nitrate, chloride and ammonium, while the respective total concentrations in gas and aerosol phases do not change. Nitrate, chloride and ammonium are thermodynamically partitioned into a gas phase and aerosol (particulate) phase in the atmosphere. The partitioning depends on temperature, humidity and the presences of other aerosol components. Focusing on acidic components, equilibrium vapor pressures between gas phase and aerosol phase are $HCl > HNO_3 > H_2SO_4$. When SO_4^{2-} concentration increases, NO_3^- and Cl^- in aerosol phase are expelled into gas phase, resulting in increased concentrations (fractions) of gaseous HNO_3 and HCl.

The deposition velocities of the highly reactive gaseous HNO_3 and HCl are high (Seinfeld and Pandis, 1998). For example, measured dry deposition velocities of HNO_3 gas are 20 times higher than those of aerosols (Brook et al., 1997). As for wet deposition, solution equilibrium Henry's law constants of HNO_3 and HCl are 2.1 x 10^5 and 727 mol/L/atm, respectively. They are extremely large compared to those of SO_2 and NO_2, 1.23 and 0.01 mol/L/atm,

respectively (Seinfeld and Pandis, 1998). Consequently, the deposition of nitrate and chloride increases as the gas-phase fractions increase due to increased SO_4^{2-}, even when the total (gas plus aerosol) concentrations do not change.

The indirect effect was prominent during extreme phenomena, for example the substantial SO_2 emissions of the Miyakejima volcano (Satsumabayashi et al., 2004, Kajino et al., 2005). The Miyakejima volcano, which has erupted continuously since July 2000, has resulted in a huge amount of SO_2 emissions to the troposphere. One year after the onset, SO_2 emissions totaled 9 Tg, amounting to half the anthropogenic SO_2 emissions from China, 20 Tg/yr. As the result, monthly mean SO_4^{2-} concentration increased by 2.5 times in Japan (Kajino et al., 2004). According to the ground based observation of gas and aerosols at the Happo Ridge observatory, located 300 km north of the Miyakejima volcano, the fractions of gaseous HNO_3 and HCl were above 95% in the Miyake-volcanic plumes, while the contaminated air masses from the continental outflow contained fractions of approximately 40%. Consequently, bimonthly mean NO_3^- and Cl^- concentrations in precipitation (wet deposition) in August and September 2000 increased by 2.7 and 1.9 times, respectively, over the same months in 1999.

In the current study, we present the indirect acidification effects under general air pollution conditions, not as a result of an extreme event such as the volcanic eruption, analyzing EANET (Acid Deposition Monitoring Network in East Asia) monitoring data. SO_x emissions from continental Asia are expected to increase in the future. Deposition of NO_3^- and Cl^- will be accelerated through the indirect acidification mechanism in areas downwind of large emission sources.

2. The monitoring network and a thermodynamic equilibrium model

2.1 EANET monitoring network.
EANET began collecting data on a regular basis in 2001. Currently, 13 countries in East and South East Asia participate, with a total of 47 wet deposition monitoring stations. In 2002, two Japanese monitoring stations began measuring concentrations
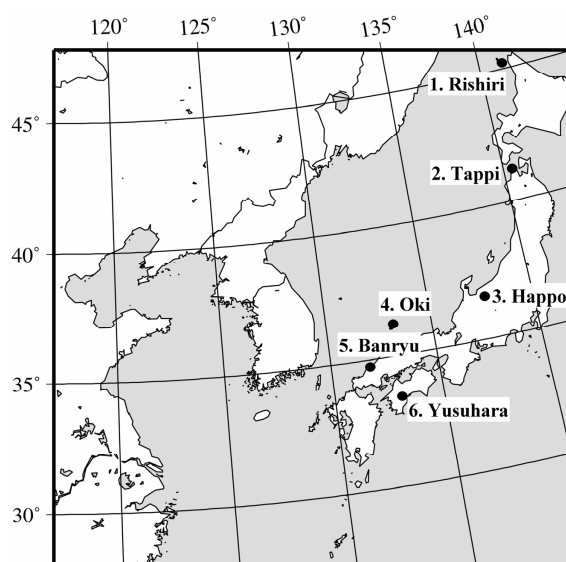

Fig. 1 Locations of 6 EANET monitoring stations in Japan. The numbers are identical to Table 1.

of gas and aerosol components for dry deposition, increasing to the current 10 stations in Japan (EANET, 2000a). These stations monitor 7 or 14-day accumulated concentrations of gaseous species (HNO_3, HCl, NH_3, SO_2) and aerosol components (SO_4^{2-}, NO_3^-, Cl^-, NH_4^+, Na^+, Mg^{2+}, K^+, Ca^{2+}) using the filter-pack method (EANET, 2003); 1-day or 7-day accumulated concentrations in precipitation (SO_4^{2-}, NO_3^-, Cl^-, NH_4^+, Na^+, Mg^{2+}, K^+, Ca^{2+}) using precipitation collection and the ion chromatography method (EANET, 2000b); and, hourly SO_2, NO, NO_2, O_3 concentrations, temperature and relative humidity.

In the present study, we used monitoring data collected at 6 Japanese stations in EANET. As shown in Fig. 1, the stations are situated along the Japan archipelago, representing various climate and air quality features from the north to southwest. Table 1 presents the monitoring results for the 6 stations. At 4 stations, Tappi, Happo, Banryu and Yusuhara, data were collected for two years from April 2003 to March 2005. At Oki, data were collected for three years beginning April 2002, and at Rishiri, for two and a half years beginning July 2002.

2.2 Multi-component gas-aerosol equilibrium model (SCAPE).
Gas-aerosol partitioning of the semi-volatile components is predicted with a multi-component thermodynamic equilibrium model using EANET

Table 1 Information and monitoring results from 6 EANET stations.

Number[a]	1	2	3	4	5	6
Name	Rishiri	Tappi	Happo	Oki	Banryu	Yusuhara
Observation period	07/2002-03/2005	04/2003-03/2005	04/2003-03/2005	04/2002-03/2005	04/2003-03/2005	04/2003-03/2005
Number of samples	72	47	46	77	47	51
Longitude	141.20	140.33	137.80	133.18	131.70	132.93
Latitude	45.12	41.25	36.70	36.28	34.68	33.37
Altitude	40m	105m	1850m	90m	53m	790m
Characteristics	Remote Marine	Remote Marine	Remote Land	Remote Marine	Urban Coast	Remote Land
Mean concentrations with standard deviations (µg/m3)						
[nss-SO$_4$]	1.86 ± 0.95	2.78 ± 2.31	2.30 ± 1.33	3.54 ± 2.05	4.12 ± 1.86	4.91 ± 1.81
[t-NO$_3$][b]	0.73 ± 0.47	1.53 ± 1.23	1.26 ± 0.74	1.21 ± 0.61	1.84 ± 0.69	1.51 ± 0.76
[t-Cl][b]	3.03 ± 1.75	12.42 ± 26.61	0.32 ± 0.11	2.31 ± 1.90	1.98 ± 1.76	0.55 ± 0.28
[t-NH$_3$][b]	0.68 ± 0.34	0.92 ± 0.60	0.89 ± 0.54	1.26 ± 0.77	1.70 ± 0.70	1.47 ± 0.52
[Minerals][c]	2.31 ± 1.26	9.89 ± 20.62	0.33 ± 0.30	2.64 ± 1.58	1.96 ± 1.06	0.90 ± 0.48
Mean meteorology with standard deviations						
T (℃)	6.50 ± 8.72	10.11 ± 7.50	4.77 ± 8.64	14.48 ± 7.17	15.21 ± 7.33	12.10 ± 7.45
RH (%)	75.69 ± 6.00	74.10 ± 8.48	79.05 ± 11.10	74.10 ± 6.16	76.76 ± 6.77	76.00 ± 7.43
Mean molar ratios with standard deviations (-)						
$C_{nssS/N5}$	1.96 ± 1.00	1.37 ± 1.28	1.31 ± 0.59	1.99 ± 1.06	1.56 ± 0.69	2.46 ± 1.26
[nss-SO$_4$]/[SO$_4$]	0.78 ± 0.13	0.65 ± 0.26	0.98 ± 0.02	0.86 ± 0.11	0.91 ± 0.08	0.98 ± 0.02
P_{gHNO3}	0.20 ± 0.16	0.27 ± 0.19	0.77 ± 0.20	0.30 ± 0.22	0.43 ± 0.27	0.70 ± 0.26
Fs	0.34 ± 0.14	0.48 ± 0.21	0.53 ± 0.17	0.37 ± 0.16	0.48 ± 0.19	0.37 ± 0.17
Correlation coefficient R (-)						
T vs. P_{g-HNO3}	0.46	0.60	0.28	0.63	0.76	0.79
$C_{nssS/N5}$ vs. P_{g-HNO3}[d]	-0.03 →0.39	0.04 →0.60	0.31	0.75	0.75	0.70
P_{g-HNO3} vs. $D_{N5/S6}/C_{N5/S6}$[d]	0.17 →0.63	-0.14 →0.34	0.21	0.74	0.58	0.41
Fs vs. $D_{N5/S6}/C_{N5/S6}$[d]	0.08 →-0.40	0.28 →-0.39	-0.29	-0.45	-0.50	-0.18

[a] Identical to Figure 1

[b] [t-NO$_3$]=[HNO$_3$]+[NO$_3^-$], [t-Cl]=[HCl]+[Cl$^-$], [t-NH$_3$]=[NH$_3$]+[NH$_4^+$]

[c] [Minerals]= [Na$^+$]+[Mg^{2+}]+[K$^+$]+[Ca^{2+}]

[d] Correlation coefficient R increased under conditions that nss-SO$_4$/SO$_4$>average and T>0 for Rishiri and Tappi

observation data. We employ the Simulating Compositions of Atmospheric Particles at Equilibrium (SCAPE) (Kim et al., 1993a, 1993b; Kim and Seinfeld, 1995; Meng et al., 1995) model in the present study. The SCAPE model calculates the thermodynamic equilibrium state among 9 inorganic aerosol components, H_2SO_4, HNO_3, HCl, NH_3, H_2CO_3, Na^+, Mg^{2+}, K^+, Ca^{2+}, under certain temperature and relative humidity conditions and predicts gas-aerosol partitioning of semi-volatile components, water uptake and aerosol acidity. The model is useful for predicting changes in gas-aerosol partitioning of nitrate, chloride and ammonium under certain hypothetical conditions, for example, if only the SO_4^{2-} concentration changes (see section 5.1), etc.

3. Indirect acidification mechanism

The indirect acidification mechanism is a process of acid deposition acceleration associated with changes in the gas-aerosol partitioning of semi-volatile aerosol components, such as nitrate, chloride and ammonium, while the respective total concentrations in gas and aerosol phases are maintained. As an example, Fig. 2 shows schematic illustrations of the indirect acidification effects on nitrate. The semi-volatile aerosol components such as nitrate, chloride and ammonium are partitioned into a gas phase and aerosol (particulate) phase in the atmosphere. Thermodynamic equilibrium is established for ammonium nitrate and ammonium chloride as follows,
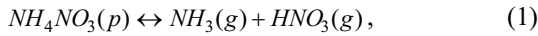
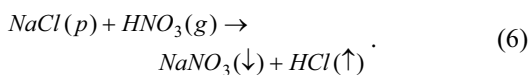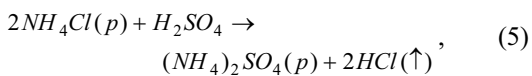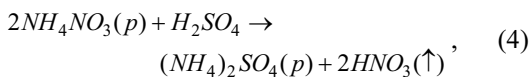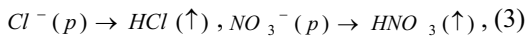Emission, transformation, transport, deposition of SO_x and NO_x
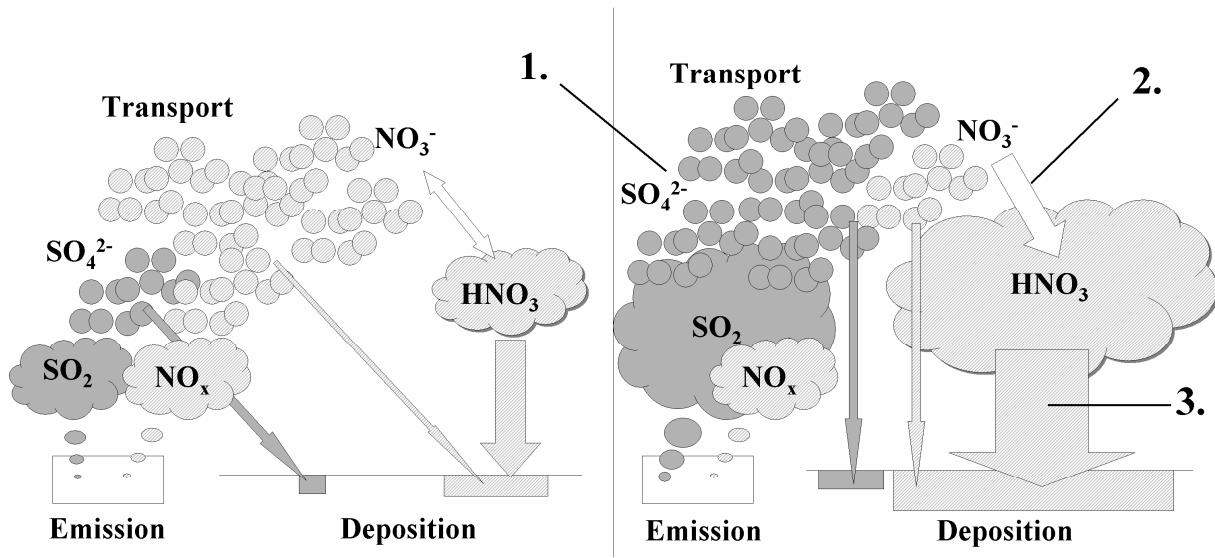
Indirect acidification
1. Increase in SO_x emission and concentration
2. Increase in gas-phase HNO_3 concentration
3. Increase in NO_3^- deposition

Fig. 2 Schematic illustration of the indirect acidification mechanism of nitrate.

$$NH_4NO_3(p) \leftrightarrow NH_3(g) + HNO_3(g), \qquad (1)$$

$$NH_4Cl(p) \leftrightarrow NH_3(g) + HCl(g), \qquad (2)$$

where (p) and (g) indicate particulate (aerosol) and gaseous phases, respectively. The partitioning is determined by temperature, humidity and the presence of other chemical components. Focusing on acidic components, equilibrium vapor pressures between the gas phase and aerosol phase are HCl > HNO_3 > H_2SO_4. NO_3^- and Cl^- in aerosol phase, for example, are evaporated under the following conditions,

$$Cl^-(p) \to HCl(\uparrow), NO_3^-(p) \to HNO_3(\uparrow), (3)$$

$$2NH_4NO_3(p) + H_2SO_4 \to \\ (NH_4)_2SO_4(p) + 2HNO_3(\uparrow), \qquad (4)$$

$$2NH_4Cl(p) + H_2SO_4 \to \\ (NH_4)_2SO_4(p) + 2HCl(\uparrow), \qquad (5)$$

$$NaCl(p) + HNO_3(g) \to \\ NaNO_3(\downarrow) + HCl(\uparrow). \qquad (6)$$

Equation 3 reflects evaporation as temperature (T) increases. The gas phase fractions of nitrate and chloride increase in summer. SO_4^{2-} is produced by atmospheric oxidizing reactions from SO_2 taking gaseous NH_3, which forms ammonium sulfate aerosols. When NH_3 gas is exhausted, SO_4^{2-} expels NO_3^- and Cl^-, changed from aerosol phase into gas phase as described by Eqs. 4 and 5. Equation 6 indicates a reaction that HNO_3 gas, deposited on sea-salt particle surfaces, expels Cl^- into gas phase.

The deposition velocities of the highly reactive gaseous HNO_3, HCl and NH_3 are high (Seinfeld and Pandis, 1998). As SO_4^{2-} concentration increases, fractions of gaseous HNO_3 and HCl concentrations increase, described in Eqs. 4 and 5, resulting in enhanced deposition of NO_3^- and Cl^- even if the total (gas plus aerosol) concentrations (t-NO_3, t-Cl) do not change. In contrast, the basic component NH_3 gas is taken into aerosol phase forming ammonium sulfate, resulting in a decrease in the gas phase fraction, which may also contribute to environmental changes.

In the current paper, we focus only on increases in wet deposition of NO_3^- due to increased SO_4^{2-} concentration. We analyze only wet deposition

because dry deposition amounts are not directly measured by EANET. Dry deposition is discussed later because of its pronounced effects on forests and farmlands. We compare the nitrate to sulfate (N/S) ratio of wet deposition with their atmospheric concentrations, and discuss the indirect acidification of NO_3^-. However, the same analysis is hardly applicable for HCl's as the process is more complex (a comparison of Cl/N, Cl/S, N/S ratios is needed). The decline in the gas-phase fraction of ammonium results in a decreased deposition flux of NH_3 gas, which may accelerate acidification. However, wet deposition flux of NH_4^+ may increase due to the substantial nucleation scavenge of ammonium, and its contribution to acidification or neutralization is not identified. Analysis of ammonium is also not discussed.

4. Sampling Results

In this section, we present the indications of indirect acidification occurrence, including increased wet deposition of NO_3^-, using the EANET monitoring data.

Table 1 summarizes information for the six Japanese monitoring stations in EANET and their corresponding monitoring data. The monitoring data, collected using the filter pack method, are analyzed and mean concentrations of nss-SO_4, t-NO_3, t-Cl, t-NH_3 and Minerals in $\mu g/m^3$ with standard deviations are shown. Nss-SO_4 indicates anthropogenic sulfate, which is defined as the difference between total SO_4 and sea-salt originated SO_4 concentrations ($=0.251 \times [Na^+]$). [ ] denotes atmospheric concentrations in $\mu g/m^3$. [t-NO_3], [t-Cl], [t-NH_3] indicates total (gas plus aerosol) nitrate ($[HNO_3]+[NO_3^-]$), chloride ($[HCl]+[Cl^-]$), ammonium ($[NH_3]+[NH_4^+]$) concentrations, respectively. [Minerals] indicates the total concentrations of cations, namely Na^+, Mg^{2+}, K^+ and Ca^{2+} (with the exception of NH_4^+). Temperature (°C) and relative humidity (%) are next. $C_{nssS/N5}$ indicates molar ratios of nss-SO_4 and N(V) concentration, namely t-NO_3 (C implies atmospheric Concentration). [nss-SO_4]/[SO_4] is an indicator of the anthropogenic air masses. P_{g-HNO3} indicates gas phase fraction of nitrate (P implies Partitioning). Fs is defined as,

$$Fs \equiv \frac{S(IV)}{S(IV)+nssS(VI)} = \frac{[S]_{SO_2}}{[S]_{SO_2}+[S]_{nss-SO_4^{2-}}}, \quad (7)$$

a ratio of tetravalent S and (tetravalent plus hexavalent) anthropogenic S, assuming that all SO_2 is anthropogenic. Low values of Fs indicate that SO_2 is sufficiently oxidized to SO_4^{2-} during long-range transport. Finally, the correlation coefficients R between sets of variables are shown. $D_{N5/S6}/C_{N5/S6}$ indicates a ratio of N/S molar ratio in precipitation and atmospheric concentration (D represents wet Deposition),

$$D_{N5/S6}/C_{N5/S6} \equiv \frac{d[NO_3^-]}{d[SO_4^{2-}]} \times \frac{[SO_4^{2-}]/96}{[HNO_3]_g/63+[NO_3^-]_p/62}, \quad (8)$$

where d[ ] denotes concentrations in precipitation ($\mu mol/L$), the subscripts g and p denote gas phase and particulate phase, respectively. As the measurement of atmospheric concentrations using the filter pack method is on a 7- and 14-day basis, the daily measured wet deposition amounts are accumulated for each station over the same sampling periods. Hourly data such as T and RH are also averaged for each period.

The six stations generally have the following features. (1) Rishiri and (2) Tappi represent relatively clean marine atmospheres and the anthropogenic indicators [nss-SO_4]/[SO_4] are less than 0.8 on average. As the counterpart of NO_3^-, mineral concentrations of Na^+ and Mg^{2+} are high (> 2 $\mu g/m^3$), resulting in low values of P_{g-HNO3} (< 0.3). The stations are located in the northern part of Japan, and temperatures drop to below 0 °C in winter. In contrast, (3) Happo and (6) Yusuhara represent inland air quality, mineral concentrations are less than 1$\mu g/m^3$ and [nss-SO_4]/[SO_4] is approximately 0.98, resulting in high values of P_{g-HNO3} (> 0.7). Happo is located in the mountainous area of Central Japan, with an altitude of 1850 m MSL, and winter temperatures are below 0 °C. (4) Oki and (5) Banryu, which are located in marine and coastal regions of western

Japan, respectively, reflect the influence of the Asian continental outflows, resulting in relatively higher values of [nss-SO$_4$]/[SO$_4$] (>0.85) and $P_{g\text{-HNO3}}$ (0.3—0.4) than Rishiri and Tappi. [Nss-SO$_4$] is greater at Oki, Banryu and Yusuhara, which are located in western Japan where the anthropogenic influence is pronounced and less at Rishiri, Tappi and Happo. No significant differences in RH are detected among the stations.

$P_{g\text{-HNO3}}$ shows positive correlations with T at all stations as indicated by the direction in Eq. 3. The correlation coefficient R between $C_{nssS/N5}$ and $P_{g\text{-HNO3}}$, indicates the expulsion as described in Eq. 4. At Oki, Banryu and Yusuhara, located in western Japan where [nss-SO$_4$] is greater than 3.5 μg/m^3, R is approximately 0.7 due to significant expulsion of NO$_3^-$ by SO$_4^{2-}$ at the stations in western Japan where the continental outflow is influential. In contrast, R is small or near zero at other stations. High altitude and low cation component concentrations at Happo result in higher values of $P_{g\text{-HNO3}}$ (>0.90 for 33% of the samples). Consequently, the correlation coefficient R between $C_{nssS/N5}$ and $P_{g\text{-HNO3}}$ is low (0.31), however the tendency is apparent in a scattergram (not shown). At Rishiri and Tappi, representing clean marine air quality, $P_{g\text{-HNO3}}$ depends mainly on T and hardly on nss-SO$_4$, and the R between $C_{nssS/N5}$ and $P_{g\text{-HNO3}}$ are –0.03, 0.04, respectively (Eq. 4 does not seem to work).

Positive correlations are obtained between $P_{g\text{-HNO3}}$ and $D_{N5/S6}/C_{N5/S6}$ at 4 stations, Oki, Banryu, Yusuhara, and Happo, corresponding to the stations where positive correlations between $C_{nssS/N5}$ and $P_{g\text{-HNO3}}$ are obtained. Here $D_{N5/S6}/C_{N5/S6}$ represents the partitioning of N(V)/S(VI) molar ratio between deposition and the atmospheric concentrations defined in Eq. 8. The higher value of $D_{N5/S6}/C_{N5/S6}$ indicates a greater N/S molar ratio in precipitation than in atmosphere, namely, greater wet deposition flux of N than of S. Accordingly, positive correlations between $P_{g\text{-HNO3}}$ and $D_{N5/S6}/C_{N5/S6}$ indicate that the wet deposition flux of nitrate becomes larger as the gas phase fraction increases, which is indirect acidification. Together with the positive correlations between $C_{nssS/N5}$ and $P_{g\text{-HNO3}}$, the expulsion of particulate NO$_3^-$ by anthropogenic SO$_4^{2-}$ to the gas phase and increased gas-phase HNO$_3$ resulting in the acceleration of the wet deposition flux are indicated

at Oki, Banryu, Yusuhara and Happo.

At Rishiri and Tappi where no correlations are detected between $C_{nssS/N5}$ and $P_{g\text{-HNO3}}$, the analysis using $D_{N5/S6}/C_{N5/S6}$ is nonsensical. The correlation coefficients R between $P_{g\text{-HNO3}}$ and $D_{N5/S6}/C_{N5/S6}$ are 0.17 and -0.14, at Rishiri and Tappi, respectively, due to the abundance of cation components originating from sea-salt particles. In addition, the indirect effect is usually based on the calculation of vapor-liquid equilibrium of semi-volatile components, however these two stations are located in the northern part of Japan where temperatures drop below 0 °C in winter and precipitation consists mostly of ice and snow, not liquid. Therefore, we selected samples under conditions that [nss-SO$_4$]/[SO$_4$] is greater than the average, reflecting a smaller influence of sea-salt particles, and mean temperature during sampling is above 0 °C. The same analysis using the conditional samples increased the correlation coefficients R between $C_{nssS/N5}$ and $P_{g\text{-HNO3}}$ from -0.03 to 0.39, 0.04 to 0.60, and R between $P_{g\text{-HNO3}}$ and $D_{N5/S6}/C_{N5/S6}$ increased from 0.17 to 0.73, -0.14 to 0.34, respectively at Rishiri and Tappi. Consequently, indirect acidification is evident under the substantial influence of anthropogenic contamination, lower influence of sea-salt particles and sufficiently high temperatures for vapor-liquid equilibrium to be established.

Figure 3 illustrates scattergrams of sampling at (4) Oki (above) and (1) Rishiri (below) started in 2002 using the filter pack. Oki, located in western Japan, is influenced by the pronounced Asian continental outflow and the correlation coefficients R are greater than at other stations. At Rishiri, located in northern Japan, the sea-salt effect is predominant and the correlations were very weak, but are enhanced significantly by sample selection under the conditions mentioned above. Figure 3 shows scattergrams between (a) $C_{nssS/N5}$ and $P_{g\text{-HNO3}}$ (%), (b) $P_{g\text{-HNO3}}$ (%) and $D_{N5/S6}/C_{N5/S6}$, (c) Fs and $D_{N5/S6}/C_{N5/S6}$ at Oki. Figures 3 (d) – (f) present the same information as (a) - (c) for Rihiri. The circles denote all samples and the closed circles in (d) - (f) denote samples under the conditions that T>0 and [nss-SO$_4$]/[SO$_4$]>average. The solid lines in (a) - (c) are regression lines of all samples, while dashed lines in (d) - (f) represent all samples (opened plus closed circles). The solid lines in (d) - (f) are the regression
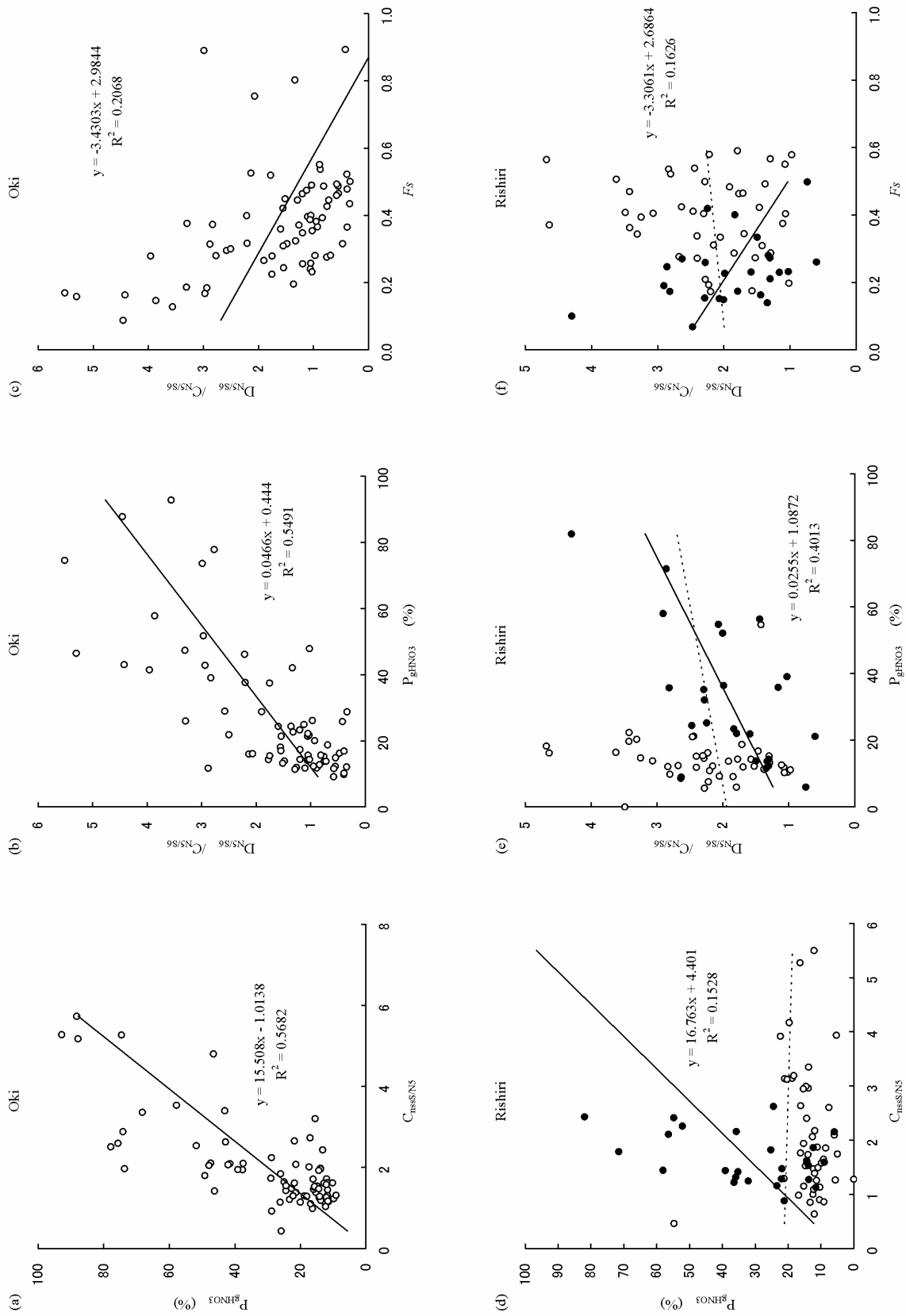
Fig. 3 Scattergrams of (a) $C_{nssS/N5}$ and $P_{g\text{-}HNO3}$, (b) $P_{g\text{-}HO3}$ and $D_{N5/S6}/C_{N5/S6}$ and (c) Fs and $D_{N5/S6}/C_{N5/S6}$ at Oki. (d) – (f) are same as (a) – (c) for Rishiri.

lines of the conditional samples (closed circles). In Fig. 3 (d) and (a), $P_{g\text{-HNO3}}$ can be greater than 50% under lower influence of sea-salt particles (closed circles) when $C_{nssS/N5}$ is less than 2 at Rishiri, while $P_{g\text{-HNO3}}$ is smaller than 30% when $C_{nssS/N5}$ is less than 2 at Oki. This is because t-NH$_3$ concentration is low at Rishiri (0.68 µg/m^3) on average, half that at Oki, which can fix NO$_3^-$ in aerosol phase. However, when cations originating from sea-salt are abundant at Rishiri (opened circles in Fig. 3d), $P_{g\text{-HNO3}}$ is smaller than 20% although $C_{nssS/N5}$ is greater than 4.

The Fs value is the indicator of an anthropogenic air mass. For the relatively short-distance transport inside Japan, the Fs value is greater than 0.6, approximately, and smaller than 0.2 for long-range transport from the continent to Japan (Satsumabayashi et al., 2004). In Fig. 3 (c), $D_{N5/S6}/C_{N5/S6}$ is greater than 3 when Fs is smaller than 0.2 and the correlation coefficient R between them is –0.45. Time series diagrams are not shown in the current paper, however the transport of the sulfate-rich contaminated continental air mass to Oki from spring to autumn results in significant indirect acidification and accelerated wet deposition of NO$_3^-$. The same trend can be seen in Fig. 3 (f) at Rishiri under a lower influence of sea-salt particles (R=-0.40). The correlation coefficients R between Fs and $D_{N5/S6}/C_{N5/S6}$ at all six stations are shown in Table 1.

5. Discussion

5.1 Indirect acidification induced by future SO$_x$ emission increases in Asia.

The Special Report on Emissions Scenarios (SRES) of the Intergovernmental Panel on Climate Change (IPCC, 2000) describes that in all four scenarios, A1, A2, B1 and B2, the rates of emissions in Asia are increasing faster than those worldwide. SO$_x$ emissions are estimated to peak between the years 2020 and 2050, becoming twice as high as in 2000. NO$_x$ emissions continue to increase after SO$_x$ cease increasing, peaking after 2040 at more than twice the present levels in the lowest estimation (B1) and by approximately 4 times in 2100 in the A2 scenario. SRES does not evaluate the increasing NH$_x$ emission rates, which affect the gas-aerosol partitioning substantially. Klimont et al. (2001)

estimated that NH$_x$ emissions will increase in East Asia by 2030 to 1.7 times 1995 levels.

The SCAPE model simulates changes in gas-aerosol partitioning of nitrate and ammonium as SO$_4^{2-}$, t-NO$_3$, and t-NH$_3$ concentrations change. The partitioning is simulated using the samples from all six EANET stations as the model input. The average and the median of the simulated $P_{g\text{-HNO3}}$ are 0.49 and 0.44, while those of the measured (monitored) $P_{g\text{-HNO3}}$ are 0.41 and 0.29, respectively. The correlation coefficient R of the modeled and the measured $P_{g\text{-HNO3}}$ is 0.70. At Oki, the average and the median of the modeled $P_{g\text{-HNO3}}$ are 0.44 and 0.31, respectively, while those of the measured are 0.29 and 0.21, respectively. The modeled values are greater than the measured ones and the correlation is not very strong (R=0.52).

If only SO$_x$ emissions increase to twice current levels on the continent (NO$_x$ and NH$_x$ emissions remain unchanged) and SO$_4^{2-}$ concentrations transported to Oki are increased by two as well, the average and the median of $P_{g\text{-HNO3}}$ using the SCAPE model are 0.72 and 0.91, respectively. Rough estimation of $D_{N5/S6}/C_{N5/S6}$ can be made from Fig. 3(b). When SO$_4^{2-}$ concentration increases by two and when $P_{g\text{-HNO3}}$ increases from 30% to 70%, $D_{N5/S6}/C_{N5/S6}$ increases by approximately two from 1.8 to 3.7 according to the regression line.

In equation 8 ($D_{N5/S6}/C_{N5/S6}$), when [SO$_4^{2-}$] is doubled, d[SO$_4^{2-}$] is assumed to be doubled, while the total [HNO$_3$]$_g$/63+[NO$_3^-$]$_p$/62 remains unchanged (only the partitioning changes). Consequently, "$D_{N5/S6}/C_{N5/S6}$ is doubled" indicates that "d[NO$_3^-$] is doubled". Although NO$_x$ emission is assumed constant, the wet deposition of NO$_3^-$ may double through the indirect acidification mechanism when SO$_4^{2-}$ concentration doubles.

Simply, but more realistically, based on the above mentioned emission scenarios, the case that [SO$_4^{2-}$], [t-NO$_3$] and [t-NH$_3$] concentrations increase by two is examined. The average and the median of the modeled $P_{g\text{-HNO3}}$ at Oki is 0.57 and 0.61, respectively. 3 mol of NH$_4^+$ is required to balance 1 mol of SO$_4^{2-}$ and 1 mol of NO$_3^-$. If those components increase together at the same rate, $P_{g\text{-HNO3}}$ increases, although the increasing ratio is smaller than the case in which [t-NH$_3$] is stable.

Thus, future increases in SO$_4^{2-}$ concentration in

Asia can induce increased wet deposition of NO_3^- in regions downwind of large emission sources through the indirect acidification processes.

5.2 Other indirect acidification effects.

Increases in SO_4^{2-} concentrations induce changes in the gas-aerosol partitioning of semi-volatile aerosol components, resulting in increases in gas phase concentrations of HNO_3 and HCl and aerosol phase concentrations of NH_4^+. Differences in the deposition velocities of gas and aerosols may change the deposition amounts of those components, subsequently. Increased wet deposition of NO_3^- is detected using the above-mentioned analysis, but to what extent does indirect acidification affect the depositions of other components?

Dry deposition velocities depend not only on components but also on meteorology and surface conditions. The dry deposition velocity of particles depends substantially on their size distribution. Consequently, estimations of the dry deposition velocities vary substantially across the targeted regions, seasons and vegetations, and the parameters used in each study. According to several measurements, the dry deposition velocity of HNO_3 gas is high (> 2cm/s) because it is highly reactive (Wesely and Hicks, 2000). The modeled dry deposition velocities of aerosols over eastern North America range from 0.1 to several cm/s (Zhang et al., 2001). The measured dry deposition velocities of NO_3^- aerosol onto the forests, where the surface resistance to dry deposition is low, are as large as several cm/s (Erisman et al., 1997, Ruijgrok, et al., 1997), however, for HNO_3 gas dry deposition velocities may be larger on the same conditions.

Simultaneous measurements of HNO_3 gas and aerosol dry deposition velocities onto the farmlands indicate that the velocities of HNO_3 are approximately 20 times larger than those of aerosols (Brook et al., 1997). This condition, for example if SO_4^{2-} concentration increases and P_{g-HNO3} increases by two from 30% to 60%, result in a forty-fold increase in dry deposition flux of HNO_3 gas.

Nitrate deposition reduces plant diversity worldwide and species richness of grasslands (Sala et al., 2000, Stevens et al., 2004). Measured dry deposition amounts of HNO_3 gas in Japanese forests and farmlands are more than twice those of NO_3^-

aerosols (Matsuda et al., 2001). Another measurement in Japanese cedar forests reported that the dry deposition amount of H^+ is greater than the wet deposition amount of H^+ throughout the year (Takahashi et al., 2001). In certain regions, seasons and vegetation, the effects of the indirect acidification on increased dry deposition of NO_3^- and consequent influence on vegetation are cause for concern.

Few studies have focused on the deposition of HCl gas. HNO_3 gas, expelled by SO_4^{2-} and deposited on aerosols, expels Cl^- into the gas phase effectively (Eq. 6). At Rishiri and Tappi, representing clean marine air, the correlation between HNO_3 gas concentration and the gas-phase fraction of HCl, P_{g-HCl} is strong (R>0.8). However, sea-salt originated Cl^- such as $NaCl$ is highly hygroscopic and act as cloud condensation nuclei (CCN), meaning that the wet deposition flux of Cl^- is largely due to nucleation scavenging in clouds. Although, increases in P_{g-HCl} cannot be shown to contribute to enhanced or reduced wet deposition of Cl^-, HCl gas is highly reactive and dry deposition velocities may be as large as those of HNO_3 gas. As a result, the indirect effects on the dry deposition of Cl^- in forests and farmlands are crucial. Chlorine emissions from sea-salt particles substantially increase ozone concentrations in coastal urban regions (Knipping and Dabdub, 2003), also inducing vegetation damage.

NH_3 gas is also highly reactive, resulting in a high deposition velocity. As NH_3 gas quickly reacts with SO_4^{2-} forming ammonium sulfate, the correlations between [nss-SO_4^{2-}] and [NH_4^+] are strong (R>0.8) at the all six stations. Increased SO_4^{2-} concentrations result in decreased NH_3 gas concentration and may cause decreases in dry deposition flux of NH_4^+. However, ammonium sulfate is also hygroscopic, so the wet deposition flux of NH_4^+ may also increase.

In order to assess all the indirect acidification effects mentioned in the present paper quantitatively, further studies are necessary using three-dimensional chemical transport models with accurate parameterizations of dry deposition velocities and precisely formulated wet deposition processes, together with regional-scale long-term monitoring data of dry and wet deposition.

5.3 Effects on the radiation budget.

Optical properties of gas and aerosols are very different. Adams et al. (2001) estimated that the radiative forcing of nitrate would be comparable to that of sulfate in the year 2100 according to the SRES A2 scenario when NO_x emissions reach 4 times 2000 levels. Schaap et al. (2007) reported that even in 1995, in Europe during the winter when the aerosol phase fraction of NO_3^- is large, the radiative forcing of nitrate amounts to half that of sulfate. Consequently, future changes in the gas-aerosol partitioning of nitrate may induce substantial change in the radiative forcing of aerosols.

6. Conclusions

Analyzing EANET monitoring data, indirect acidification, the enhancement of NO_3^- wet deposition associated with increases in SO_4^{2-} was revealed under general air pollution conditions. The indirect acidification is most influential from spring to autumn in western Japan when the Asian continental outflow carries sulfate-rich contaminated air masses, but is not pronounced in the air masses containing abundant sea-salt particles and related increases in aerosol cation components.

When the sulfate concentration doubles, wet deposition of NO_3^- is found to possibly double as well even when NO_x emissions, and subsequent total nitrate concentrations, remain unchanged. In areas, such as forests, where surface resistance is low, dry deposition of NO_3^- is more pronounced than the wet deposition. Increases in dry deposition of NO_3^- due to the indirect effect are of great concern in such regions because the dry deposition velocity of HNO_3 gas is very high. The deposition of other semi-volatile components, such as chloride and ammonium, also can be changed through the indirect acidification mechanism. To evaluate all those effects, further studies are necessary using three-dimensional chemical transport models.

The filter pack method with 14-day accumulated measurements, performed by EANET, was used in this study. In this method, one sample does not represent a single event but represents the averages of different air masses, as several meteorological systems might pass the monitoring sites during a long period of 14 days. Consequently, the atmospheric chemical composition measured by the filter pack method and in precipitation sampled on a daily basis, may originate from different air masses (it is still meaningful that certain correlations were found in the current analysis). Thus, precise wet deposition fluxes and wet scavenging coefficients from this measurement could not be derived. Further observational studies would be interesting, investigating relationships between gas-aerosol partitioning and the wet scavenging coefficients of nitrate derived from measurements with finer time resolutions (ex., 6-hour simultaneous sampling of gas, aerosols and precipitation).

References

Adams, P.J., J.H. Seinfeld, D. Koch, L. Mickley, D. Jacob (2001): General circulation model assessment of direct radiative forcing by the sulfate-nitrate-ammonium-water inorganic aerosol system, J. Geophys, Res,. Vol. 106(D1), pp. 1097—1111.

Brook, J.R., F. Di-Giovanni, S. Cakmak, T.P. Meyers (1997): Estimation of dry deposition velocity using inferential models and site-specific meteorology –uncertainty due to siting of meteorological towers, Atmos. Environ., Vol. 31, No. 23, pp. 3911—3919.

EANET (2000a): "Guidelines for Acid Deposition Monitoring in East Asia".
  http://www.eanet.cc/product.html

EANET (200b): "Technical Documents for Wet Deposition Monitoring in East Asia"
  http://www.eanet.cc/product.html

EANET (2003): "Technical Documents for Filter Pack Method in East Asia"
  http://www.eanet.cc/product.html

Erisman, J.W., G. Draaijers, J. Duyzer, P. Hofschreuder, N. van Leeuwen, F. Romer, W. Ruijgrok, P. Wyers, M. Gallagher (1997): Particle deposition to forests –summary of results and application, Atmos. Environ., Vol. 31 No. 3, PP. 321—332.

Finlayson-Pitts, B.J., J.N. Pitts Jr. (1997): Tropospheric air pollution: ozone, airborne toxics, polycyclic aromatic hydrocarbons, and particles, Science, pp. 1045—1052.

IPCC, 2000: Special Report on Emissions Scenarios [Nakicenovic, N. (eds.)]. Cambridge University Press, Cambridge, United Kingdom and New York,

NY, USA, 599 pp.

Jang, M., N.M. Czoschke, L. Sangdon, R.M. Kamens (2002) Heterogeneous atmospheric aerosol production by acid-catalyzed particle-phase reactions, Science, Vol. 298, pp. 814—817.

Kajino, M., H. Ueda, H. Satsumabayashi, J. An (2004): Impacts of the eruption of Miyakejima Volcano on air quality over far east Asia, J. Geophys. Res., Vol. 109, D21204, doi:10.1029/2004 JD004762.

Kajino, M., H. Ueda, H. Satsumabayashi, Z. Han (2005): Increase in nitrate and chloride deposition in east Asia due to increased sulfate associated with the eruption of Miyakejima Volcano, J. Geophys. Res., Vol. 110, D18203, doi:10.1029/2005JD00 5879.

Klimont, Z., J. Cofala, W. Schopp, M. Amann, D.G. Streets, Y. Ichikawa, S. Fujita (2001) Projections of SO_2, NO_x, NH_3 and VOC emissions in East Asia up to 2030, Water, Air, and Soil Pollution, Vol. 130, pp. 193—198.

Kim, Y.P., J.H. Seinfeld, P. Saxena (1993a): Atmospheric gas-aerosol equilibrium: I. Thermodynamic model. Aerosol Sci. Tech., Vol. 19, pp. 157—181.

Kim, Y.P., J.H. Seinfeld, P. Saxena (1993b): Atmospheric gas-aerosol equilibrium: II. Analysis of common approximations and activity coefficient calculation methods. Aerosol Sci. Tech., Vol. 19, pp. 182—198.

Kim, Y.P. and J.H. Seinfeld (1995): Atmospheric gas-aerosol equilibrium: III. Thermodynamics of crustal elements Ca^{2+}, K^+ and Mg^{2+}, Aerosol Sci. Tech., Vol. 22, pp. 93—110.

Knipping, E.M., D. Dabdub (2003): Impact of chlorine emissions from sea-salt aerosol on coastal urban ozone, Environ. Sci. Tech., Vol. 37, pp. 275—284.

Laskin, A., D.J. Gaspar, W. Wang, S.W. Hnut, J.P. Cowin, S.D. Colson, B.J. Finlayson-pitts (2003): Reactions at interfaces as a source of sulfate formation in sea-salt particles, Science, Vol. 301, pp. 340—344.

Matsuda, K., N. Fukuzaki, M. Maeda (2001): A case study on estimation of dry depsosition of sulfur and nitrogen compounds by inferential method, Water, Air, and Soil Pollution, Vol. 130, pp. 553-558.

Meng, Z., J.H. Seinfeld, P. Saxena, and Y.P. Kim (1995): Atmospheric gas-aerosol equilibrium: IV. Thermodynamics of Carbonates. Aerosol Sci. Tech., Vol. 22, pp. 131—154.

Ravishankara, A.R. (1997): Heterogeneous and multiphase chemistry in the troposphere, Science, Vol. 276, pp. 1058—1065.

Ruijgrok, W, H. Tieben, P. Eisinga (1997): The dry deposition of particles to a forest canopy: a comparison of model and experimental results, Atmos. Environ., Vol. 31, No. 3, pp. 399—415.

Sala, O.E., F.S. Chapin III, J.J. Armesto, R. Berlow, J. Bloomfield, R. Dirzo, E. Huber-Sanwald, L.F. Huenneke, R.B. Jackson, A. Kinzig, R. Leemans, D. Lodge, H.A. Mooney, M. Oesterheld, N.L. Poff, M.T. Sykes, B.H. Walker, M. Walker, D.H. Wall (2000): Global biodiversity scenarios for the year 2100, Science, Vol. 287, pp. 1770—1774.

Satsumabayashi, H., M. Kawamura, T. Katsuno, K. Futaki, K. Murano, G.R. Carmichael, M. Kajino, M. Horiguchi, H. Ueda (2004): Effects of Miyake volcanic effluents on airborne particles and precipitation in central Japan, J. Geophys. Res., Vol. 109, D19202, doi:10.1029/2003JD004204.

Schaap, M., F. Sauter, P. Builtjes (2007): On the direct aerosol forcing of nitrate over Europe –Simulation with the new LOTOS-EUROS model, Proceedings of 28th NATO/CCMS International Technical Meeting on Air Pollution and its Application, in press.

Stevens, C.J., N.B. Dise, J.O. Mountford, D.J. Gowing (2003): Impact of Nitrogen Deposition on the Species Richness of Grassland, Science, Vol. 303, pp. 1876—1879.

Seinfeld, J.H., S.N. Pandis (1998): Atmospheric Chemistry and Physics, from Air Pollution to Climate Change, John Wiley, New York, 430 pp.

Takahashi, A., K. Sato, T. Wakamatsu, S. Fujita (2001): Atmospheric deposition of acidifying components to a Japanese cedar forest, Water, Air, and Soil Pollution, Vol. 130, pp. 559—564.

Wesely M.L., B.B. Hicks (2000) A review of the current status of knowledge on dry deposition, Atmos. Environ., Vol. 34, pp. 2261—2282.

Zhang, L., S. Gong, J. Padro, L. Barrie (2001): A size-segregated particle dry deposition scheme for an atmospheric aerosol module, Atmos. Environ., Vol. 35, pp. 549—560.

アジア域における間接的酸性化効果：
硫酸によりエアロゾル相から追い出された硝酸ガスによる沈着の促進

梶野瑞王*・植田洋匡**・仲山伸次**・石川裕彦

*京都大学防災研究所 COE 研究員
**酸性雨研究センター

要旨

　東アジア酸性雨モニタリングネットワーク(EANET)の国内 6 地点の観測結果から，間接的酸性化効果が越境大気汚染に伴い生じている事が分かった。SO_4^{2-}濃度増加に伴いエアロゾル中の NO_3^- が追い出され，HNO_3ガス濃度が増加する。 HNO_3ガスの沈着速度は非常に速いので，結果としてトータル（ガス状＋エアロゾル状）の NO_3^-濃度が変化しなくても，NO_3^-の沈着量が増加する事になる。西日本の日本海側では，アジア大陸からのアウトフローの影響下で間接的酸性化効果は顕著になり，一方，海塩粒子が豊富にある冬季日本海側ではこの効果はあまり見えなかった。

キーワード：酸性沈着，硫酸，硝酸，乾性沈着，湿性沈着